Optical model description of anomalous elastic and inelastic α-^{40}Ca scattering between 20 and 50 MeV

F. Michel and R. Vanderpoorten*
Faculté des Sciences, Université de l'Etat, 7000 Mons, Belgium
(Received 27 December 1976)

An optical model analysis of the anomalous large angle elastic α-^{40}Ca scattering between 20 and 50 MeV has been performed on the basis of a single fit at 29 MeV incident energy. The resulting potential gives a good description of the characteristic energy dependence of the angular distributions. A nonresonant interpretation of the phenomenon is proposed. A distorted wave Born approximation analysis of some inelastic transitions is presented.

[NUCLEAR REACTIONS ^{40}Ca(α,α), ^{40}Ca(α,α'), E=20–50 MeV; calculated $\sigma(\theta)$; optical model analysis; DWBA analysis.]

I. INTRODUCTION

Much time has elapsed since the first experimental evidences of the anomalous character of the large angle elastic α-particle scattering from some light- and medium-weight nuclei (ALAS) have been reported; although many efforts have been continuously devoted to the study of the phenomenon, no clear-cut picture of the underlying mechanism has emerged as yet.[1,2]

None of the many theoretical models put forward to explain ALAS around $A \simeq 40$ has up to now succeeded in giving a quantitative—or at least semiquantitative—description of the unmistakable energy dependence of the anomalous angular distributions in the backward hemisphere.[3-6] Many data have however been gathered in the last ten years, and enough material has now become available to attempt a global analysis of the data over an extended energy range and "substantially eliminate the confusion and often totally erroneous conclusions which result from theoretical study of isolated angular distributions," as pointed out by Gobbi *et al.*[7] for heavy ion scattering. It should be noted in this respect that a recent high resolution study of Eberhard *et al.*[8] indicates that statistical fluctuations persist for ^{40}Ca(α,α) up to at least 27 MeV incident energy.

All the early optical model analyses of ALAS in the $A \simeq 40$ mass region (to which we restrict ourselves in this paper) resulted in unusual values of the parameters of the real potential well, i.e., radii and diffusenesses respectively smaller and larger than those used for normal targets,[9-12] and aroused suspicion on the feasibility of a potential explanation of the backward enhancement in this mass region. However, simple folding model ideas suggest that the presence of α correlations in the low density region of the target nucleus could affect the direct part of the α-target interaction in the surface region[13] to which the calculated angular distributions are known to be very sensitive at low energies, and explain the anomalous values assumed by the parameters in optical model analyses of ALAS (the plausibility of the cluster hypothesis and its ability to account for the strong isotope effect showing up in ALAS have been thoroughly discussed by the Heidelberg group[6,14,15]). Encouraged by the success of calculations based on the crude semimicroscopic approach developed in Ref. 13, we have extended the optical model analysis of anomalous elastic α-particle scattering from ^{40}Ca to the energy range 20 to 50 MeV: the optical parameters were adjusted to the experimental 29 MeV elastic scattering data,[6] and the resulting potential was kept fixed at all other energies except for a linear increase of the radius of its imaginary part. The results of our analysis are presented and discussed in Sec. II. Section III is devoted to a conventional distorted wave Born approximation (DWBA) analysis of inelastic ^{40}Ca(α,α') data extending up to large angles in the investigated energy range, i.e., those of the Heidelberg group at 29 MeV,[16] of the Munich group at 24 MeV,[17] as well as a sample of new data obtained at Louvain-la-Neuve between 40 and 62 MeV.[18]

II. ANALYSIS OF THE ELASTIC SCATTERING DATA

A. Experimental situation

In this subsection, we recall very briefly the salient features of the anomalous ^{40}Ca(α,α) differential cross sections at low energies, with particular emphasis on the characteristic energy behavior of the angular distributions in the backward hemisphere.

One of the most striking peculiarities of the large angle oscillations pointed out in the early experimental investigations is the fast variation of their amplitude with energy; however, the angular position of the backward maxima was shown to remain relatively fixed over wide energy ranges, in contrast to that of the forward-angle pattern which regularly shifts to small angles according to the usual diffraction theory as the incident energy is increased.[4,19,20] Exceptions to this empirical rule are observed around 20,[6] 30,[3,4] and 45 MeV[5]; at these energies, a sudden change in the position of the backward oscillations is observed together with a rapid increase in the slope of their envelope: This contrasts to the continuously decreasing behavior of this slope at other energies (see, e.g., Figs. 4 and 5). The data of the Berkeley group[5] show no further discontinuity of this type beyond 45 MeV: The slope of the large angle envelope continuously decreases up to the highest investigated energies; this has been confirmed by the recent measurements of the backward angle ^{40}Ca(α,α) differential cross sections up to 62 MeV at Louvain-la-Neuve.[18]

Prominent structures, several MeV wide, show up in the large angle excitation function; their maxima are located for ^{40}Ca around 22 and 31 MeV.[3,21,22] A recent extention of the measurements up to 66 MeV incident energy (Louvain-la-Neuve–Mons collaboration) has revealed the existence of a broad plateau around 45 MeV incident energy.[23]

B. Optical model analysis of the elastic scattering cross sections between 20 and 50 MeV

In order to gain additional flexibility in the surface region of the potential to which the α-target interaction is most sensitive at low energies (see, e.g., Ref. 24), we decided to modify the conventional Woods-Saxon geometry; this led us to the choice of some real adjustable power of the Woods-Saxon form factor:

$$f(r;R,a,\nu)=\{1+\exp[(r-R)/\nu a]\}^{-\nu}\ , \qquad (1)$$

which contains but one additional parameter. Form factors of this type (with $\nu=2$) have been used successfully in the analysis of α-particle elastic scattering data at low[25,26] as well as high energies[27]; their radial dependence is very similar to that of potentials calculated in the frame of the folding model[28] which has been shown to be especially appropriate for strongly absorbed projectiles (see, e.g., Ref. 29 and references therein). As the calculated angular distributions do not markedly depend on the details of the imaginary part of the potential[24] and in order to keep the number of variable parameters to a minimum, use was made of identical real and imaginary geometries:

$$U(r)=(V_0+iW_0)f(r;R,a,\nu)+V_C(r)\ ; \qquad (2)$$

$V_C(r)$ denotes the usual Coulomb potential due to a uniformly charged sphere of radius $1.3A^{1/3}$ fm.

The five parameters V_0, W_0, R, a, and ν were adjusted to the experimental data of Gaul *et al.*[6] at 29 MeV incident energy; the fit was performed by means of an automatic search procedure in order to minimize the quantity

$$\Delta^2=\frac{1}{N}\sum_{i=1}^{N}\left[\frac{\sigma_{\rm th}(\theta_i)-\sigma_{\rm exp}(\theta_i)}{\Delta\sigma(\theta_i)}\right]^2, \qquad (3)$$

where $\sigma_{\rm th}(\theta_i)$ is the theoretical cross section at angle θ_i, $\sigma_{\rm exp}(\theta_i)$ is the experimental cross section at θ_i, and $\Delta\sigma(\theta_i)$ is related to the error in $\sigma_{\rm exp}(\theta_i)$ and takes into account the error on angle θ_i. No attempt to search the usual potential ambiguities was made in this work. Potential No. 4 used by Budzanowski *et al.* in their investigation of ^{39}K(α,α) anomalous scattering around 25 MeV (hereafter referred to as the Cracow potential)[11] was chosen as a starting point in parameter space; the search resulted in the following values:

$$\begin{aligned} &V_0=-287.9\ \text{MeV},\\ &W_0=-29.9\ \text{MeV},\\ &R=4.87\ \text{fm},\\ &a=0.56\ \text{fm},\\ &\nu=2.65. \end{aligned} \qquad (4)$$

The real part of the corresponding potential is very similar in the surface region (say, from 5 to 8 fm) to that of the Cracow potential and that built in an earlier semimicroscopic calculation of Ref. 13. This is displayed in Fig. 1 where we have also plotted the real part of the folded potential used in the analysis of ^{44}Ca(α,α) elastic scattering between 18 and 49.5 MeV[30] which is known to be free from any backward anomaly[6,30,31]: The slope and depth of the latter potential markedly differ in the outside region from their anomalous counterparts. The calculated angular distribution corresponding to the parameter set (4) appears in Fig. 2 which reveals quite a satisfactory agreement with experiment, especially with regard to the position and slope of the backward oscillations.

We then investigated the two nearby energies 27 and 31 MeV[3] with the same values of the parameters; as can be seen in Fig. 3, the experimental angular distributions undergo a spectacular change in this restricted energy range. This peculiar behavior is nicely described by our calculation; in particular, it is comforting to note that the model adequately describes the sudden jump observed in

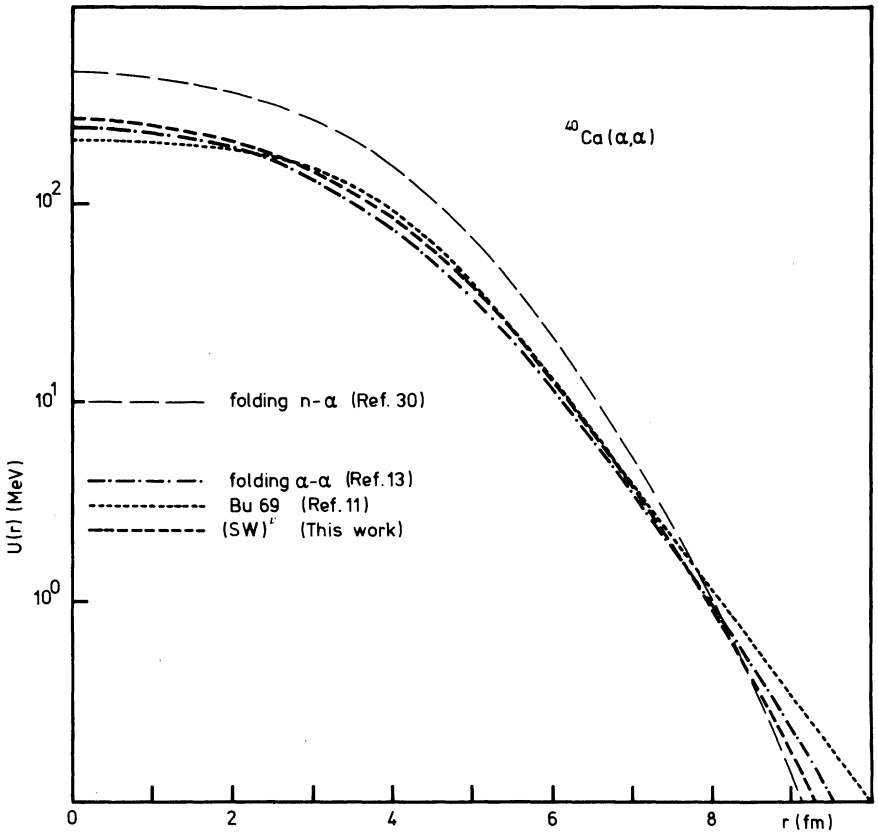

FIG. 1. Comparison of potential (4) with various α-^{40,44}Ca interactions taken from Refs. 11, 13, and 30.

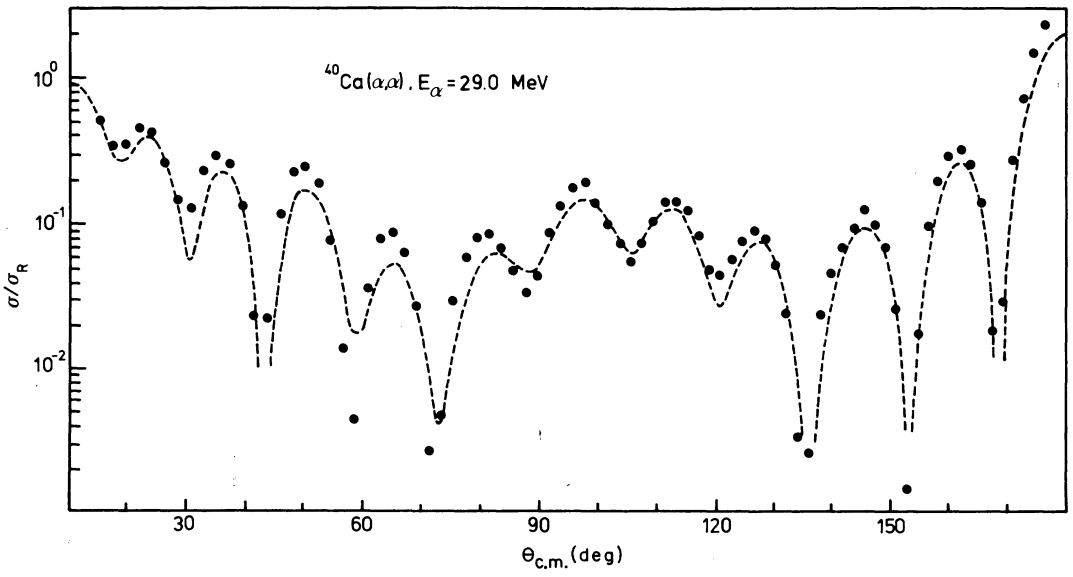

FIG. 2. Fit to the 29 MeV ^{40}Ca(α, α) experimental angular distribution corresponding to the parameter set (4).

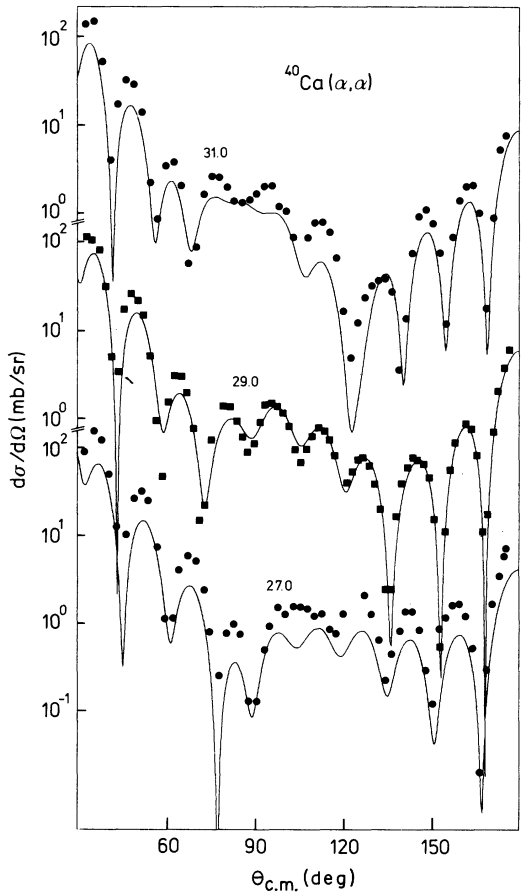

FIG. 3. Comparison of the ^{40}Ca(α,α) experimental data at 29 MeV (Ref. 6) and at 27 and 31 MeV (Ref. 3) with the predictions of the parameter set (4).

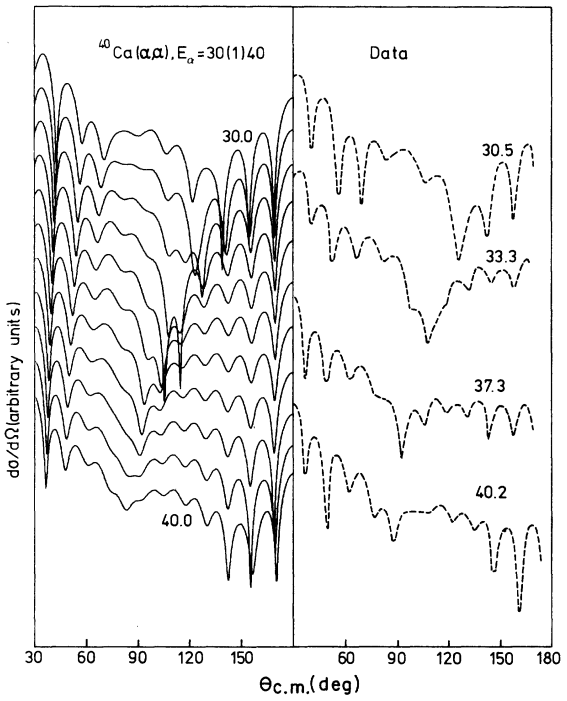

FIG. 4. Comparison of the ^{40}Ca(α,α) experimental data between 30.5 and 40.2 MeV (Ref. 4) with the predictions of the energy-dependent potential of (4) and (5) between 30 and 40 MeV in 1 MeV steps.

the angular position of the experimental backward oscillations, which had remained practically fixed over some 5 MeV in the 22–27 MeV range.[6,20]

To further check the physical significance of our optical model approach to ALAS, we next studied the experimental data of Gruhn and Wall at 30.5, 33.3, 37.3, and 40.2 MeV.[4] In order to take into account the progressive opening of new nonelastic channels with increasing energy, the radius of the imaginary part of our potential was allowed to vary linearly with energy according to

$$R_w = (3.853 + 0.035E_\alpha)\ \text{fm}, \qquad (5)$$

which for $E_\alpha = 29$ MeV coincides with the value $R = 4.87$ fm of set (4). The energy-dependent potential of (4) and (5) was used to generate the theoretical curves of Fig. 4 in 1 MeV steps between 30 and 40 MeV; this figure gives a fair illustration of the constancy of the angular position of the calculated oscillations in the backward hemisphere from 31 to 39 MeV as compared with the very systematic shifting of the diffraction maxima with increasing energy. Particularly noticeable too are (i) the regularly decreasing slope of the envelope of the large angle oscillations; (ii) the occurrence of a dip at intermediate angles whose position shifts to smaller angles as the energy increases; (iii) the progressive filling up of the backward minima from 30 up to about 35 MeV, followed by their deepening at higher energies.

A careful examination of Fig. 4 reveals that these predictions are in good semiquantitative agreement with experiment at all energies. It should be noted in this respect that no variation of the parameters (except R_w) was involved in these calculations and that better fits can be obtained at the expense of small parameter variations at individual energies; however, it was felt that this was not desirable at this stage as this would obscure our analysis.

Finally, we extended the calculations to the range 20 to 50 MeV incident energy; comparison of the predictions of the model with experiment at selected energies appears in Fig. 5: Comments similar to those made at lower energies will not be repeated here. We only want to point out the correctness of the angular position of the calculated

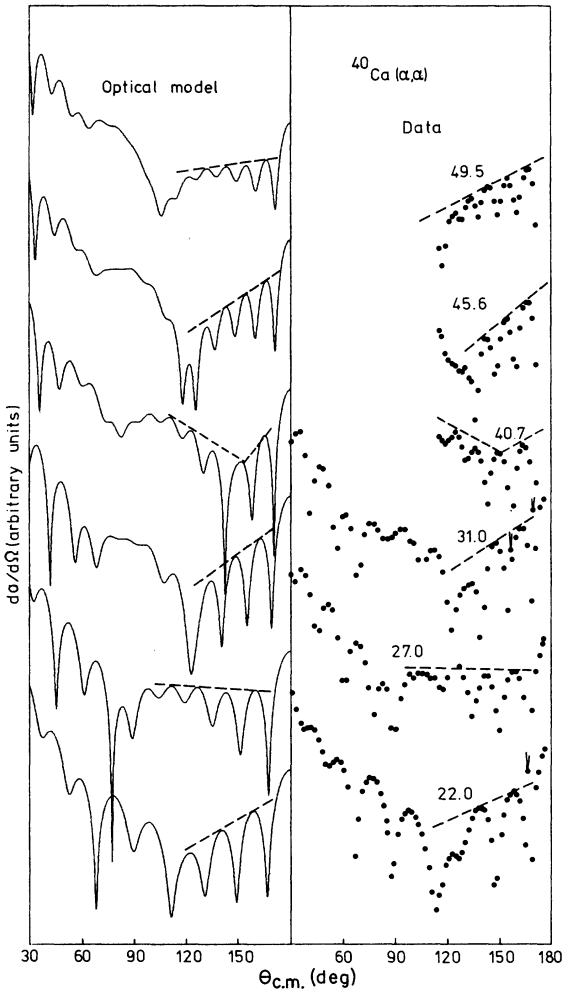

FIG. 5. Comparison of the $^{40}Ca(\alpha,\alpha)$ experimental data at 22 MeV (Ref. 6), 27 and 31 MeV (Ref. 3), and 40.7, 45,6 and 49.5 MeV (Ref. 5) with the predictions of the energy-dependent potential of (4) and (5); the dotted lines are drawn to guide the eye along the envelope of the backward oscillations.

backward oscillations at all the investigated energies, and in particular of their constancy in the ranges 22–27 MeV, 31–39 MeV, and about 42 MeV onward. We also would like to insist on the fact that occasional discrepancies between theory and experiment in the intermediate region ($100° \lesssim \theta \lesssim 130°$) are by no means essential, as the calculated cross sections are very sensitive there to minor changes of both the input parameters and the incident energy; this sensitivity results from the delicate interplay of the contributions of the wave reflected at the Coulomb barrier and that passing through this barrier and reemerging after one internal reflection, as shown in a recent semiclassical study of barrier penetration effects by Brink and Takigawa.[32]

Calculations carried out with the same potential at higher energies ($E_\alpha \lesssim 60$ MeV) predict a rapid decrease of the slope of the envelope of the back-angle oscillations, in qualitative agreement with the new data obtained at Louvain-la-Neuve.[18] However, the agreement with experiment deteriorates as the energy increases, which might point to the need for a variation of the real potential strength over an energy range of some 40 MeV or more,[33] or reflect the inadequacy of our potential in the inside region to which the scattering becomes increasingly sensitive at higher energies[34,35]; in fact, the depth of our real well exceeds by far that of the unique potential subsisting at incident energies which allow the resolution of the familiar optical model family ambiguities.[33]

Calculation of the elastic excitation function for $\theta = 180°$ was carried out with the energy-dependent potential of (4) and (5) in the range 20–55 MeV; the theoretical curve is compared with experimental data taken close to 180° in Fig. 6. Inspection of the figure shows that the position as well as width of the first two experimental bumps are well described by the model; moreover, the rapid decrease of the experimental cross section observed around 35 MeV stops at 38 MeV and is followed by a wide plateau, in qualitative agreement with the predictions of the calculation. However, from about 40 MeV onward, the quality of the description progressively deteriorates, again suggesting comments similar to those made at the end of the preceding paragraph.

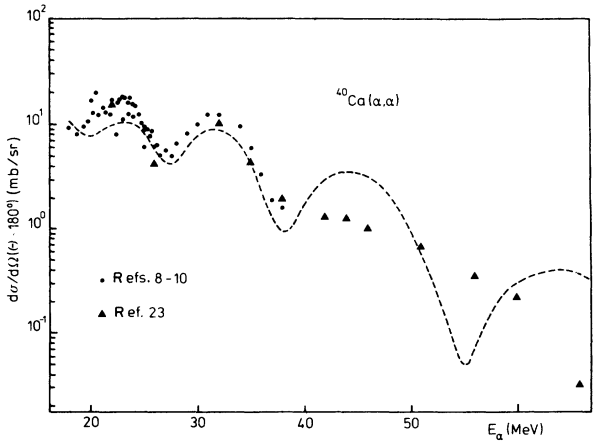

FIG. 6. Large angle experimental excitation function (Refs. 8, 9, 10, and 23) vs predictions of the energy-dependent potential of (4) and (5) at $\theta = 180°$.

C. Behavior of the scattering reflection coefficients in the investigated energy range

Examination of the reflection coefficients reveals that the gross structure of the backward-angle excitation function is not related to single particle shape resonances developing inside the "potential pockets" of the combined nuclear, centrifugal, and Coulomb potential. This structure thus seems to be very similar to that observed in elastic α-particle scattering from well-behaved targets such as Ni, Co, and Cu, which is conveniently described in the frame of a conventional optical model approach[36,37]: The analysis reveals that the bumps observed in the large angle excitation function result from a coherent superposition of several partial waves which do not display a resonant behavior.[36]

To illustrate the nonresonant nature of ALAS in the $A=40$ mass region, simple numerical experiments were carried out with the energy-dependent potential of (4) and (5). We first calculated the elastic excitation function at $\theta=180°$ between 20 and 50 MeV for increasing depths of the imaginary part of the potential. Many resonances corresponding to short-lived quasibound or virtual states appear when the absorption is turned off: the narrowest of them can be directly identified in the calculated excitation function (Fig. 7); the others are detected by inspection of the energy behavior of the reflection coefficients. Figure 8 displays the $l=13$ reflection coefficient for energies ranging from 25 to 35 MeV, together with the modulus of $(\eta_{13}-1)$ which gives a direct measure of the contribution to the scattering amplitude of the $l=13$ partial wave resonating at about 30 MeV incident energy.

Now, if the absorption is progressively turned on, the trajectories of the reflection coefficients correspondingly deviate from the unit circle and a rapid vanishing of the resonant maxima is observed (Figs. 7 and 8); these are replaced by broader structures whose peak to valley ratios tend to increase with absorption (see also Ref. 36). Inspection of Fig. 8 shows that from about $|W|=20$ MeV onward, the energy behavior of the reflection coefficients closely resembles that predicted by conventional strong absorption models such as that of Frahn and Venter.[38]

To elucidate the physical origin of these new structures, we decomposed the complex scattering amplitude for $\theta=180°$ in its real and imaginary components; this decomposition is displayed in Fig. 9(a) for energies ranging between 20 and 30 MeV: This figure indicates that the structure observed in the excitation function mainly results from a corresponding variation of the imaginary part of

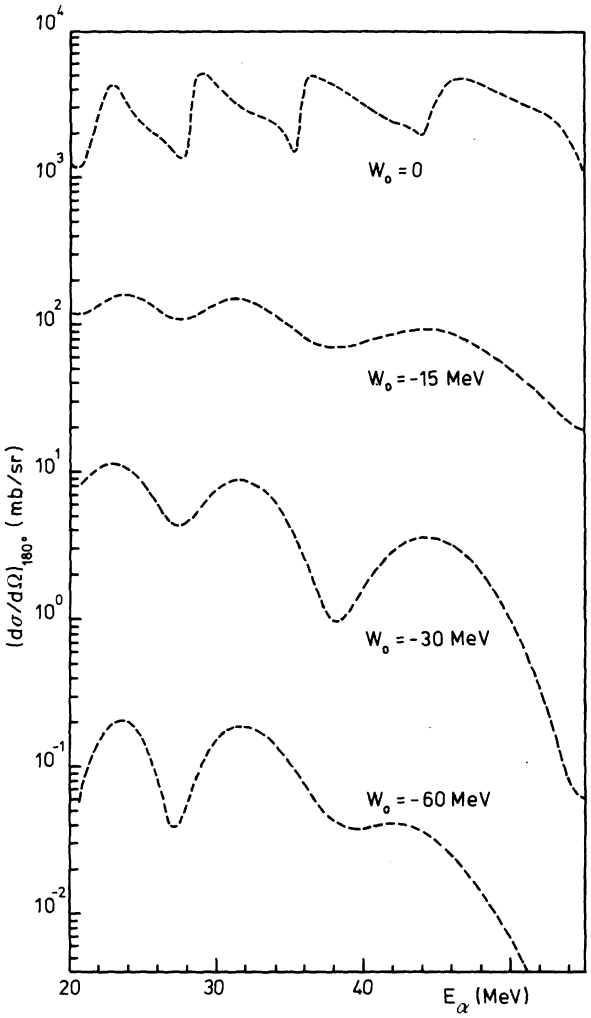

FIG. 7. Elastic $^{40}Ca(\alpha,\alpha)$ excitation function calculated at $\theta=180°$ for increasing depths of the imaginary part of the potential of (4) and (5).

the scattering amplitude. The latter was then split into its various angular momentum components $\mathrm{Im}f_l$ $(\theta=180°)$; components showing a significant variation in the investigated energy range (i.e., those whose angular momentum is near to kR, where R is a distance of the order of the nuclear radius) are displayed in Fig. 9(b), as well as the result of selective summations over angular momentum. This figure shows clearly how interference between the contributions of adjacent partial waves of angular momenta ranging from about 9 to 14 accounts for the bump observed in the imaginary part of the total complex amplitude (solid line); similar results have been shown to hold at higher energies.[39] Our interpretation is consistent with both the partial wave analysis of optical model

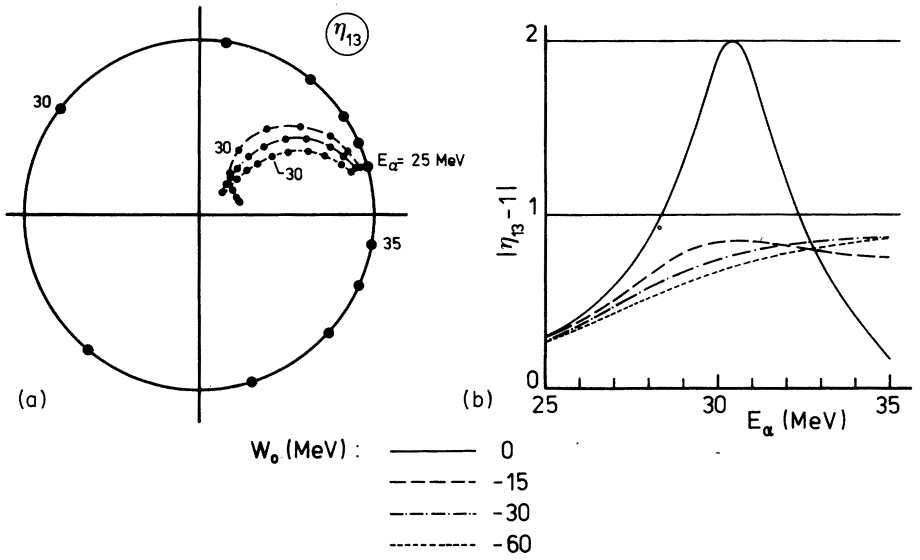

FIG. 8 (a) Behavior of the $l=13$ reflection coefficient for energies ranging from 25 to 35 MeV for various depths of the imaginary part of the potential. (b) Energy behavior of $|\eta_{13}-1|$.

calculations performed by the Cracow group[36,37] and the recent investigation of the calcium case by Brink, Grabowski, and Vogt[40] in the frame of their semiclassical approach to the study of barrier penetration effects[32] (cf. supra); in the latter work, the structures observed in the backward-angle excitation function when strong absorption is effective are discussed in terms of the interference between the internal and barrier-reflected waves.

We also would like to discuss the quasimolecular picture of the ALAS phenomenon for $A \simeq 40$[5,41] which has recently been investigated from a microscopic point of view in the frame of the resonating group method.[42,43] This resonant interpretation is supported by the fact that, at some energies, angular distributions are well represented by the square of a single Legendre polynomial in the backward hemisphere; moreover, plotting these energies against the extracted l values in a $[E_x, l(l+1)]$ diagram (where E_x denotes the excitation energy of the compound system) nearly gives a straight line. This behavior could be a mere reflection of the strong absorption encountered in elastic α-particle scattering at low energies.[44,45] As a matter of fact, the α-target interaction is characterized by the so-called strong absorption radius $R_{1/2}$ (see, e.g., Ref. 46), which is fairly energy independent.[47] If η_l denotes the lth scattering reflection coefficient, this radius is related to the cutoff angular momentum L_0 for which $\mathrm{Re}\eta_l = \frac{1}{2}$ by the relation[46]:

$$E_{\mathrm{c.m.}} \equiv E_x - Q \simeq \frac{\hbar^2}{2\mu R_{1/2}^2} L_0(L_0+1) + \frac{Z_1 Z_2 e^2}{R_{1/2}}, \quad (7)$$

where the various symbols have their usual meaning. If the transition in angular momentum space between strongly absorbed partial waves ($|\eta_l| \simeq 0$) and nearly completely transmitted ones ($|\eta_l| \simeq 1$) is steep enough, then the large angle angular distributions will exhibit backward oscillations which can approximately be represented by the square of a Legendre polynomial of order $L \simeq L_0$; in fact, in the limit of the sharp-cutoff model, it can be shown that at large angles

$$\sum_{l=0}^{L_0} (2l+1) P_l(\cos\theta) \simeq (L_0+1) P_{L_0}(\cos\theta). \quad (8)$$

Current estimates of the strong absorption radius for ^{40}Ca lie around 7 fm[46,48]; insertion of $R_{1/2} = 6.4$ fm into Eq. (7) gives

$$E_x = 0.14 L_0(L_0+1) + 14 \text{ MeV}, \quad (9)$$

that is, values of the slope and "bandhead" energy very near the experimental values (due to the roughness of our estimations, the value $R_{1/2} = 6.4$ fm is in reasonable agreement with the above-mentioned experimental values). In this picture, the localization of the bandhead above the ^{44}Ti ground state is interpreted as a mere Coulomb effect.

Finally, we examined the reflection coefficients generated by the l-dependent optical potential of Eberhard[49] at 24 MeV: they turned out to differ considerably from those obtained from the potential of (4) and (5), especially for low l values. Any modification of the optical potential coefficients is likely to strongly affect the large angle behavior of the elastic cross section because of the strong cancellations between the individual partial wave amplitudes occurring near $\theta = 180°$. In the l-de-

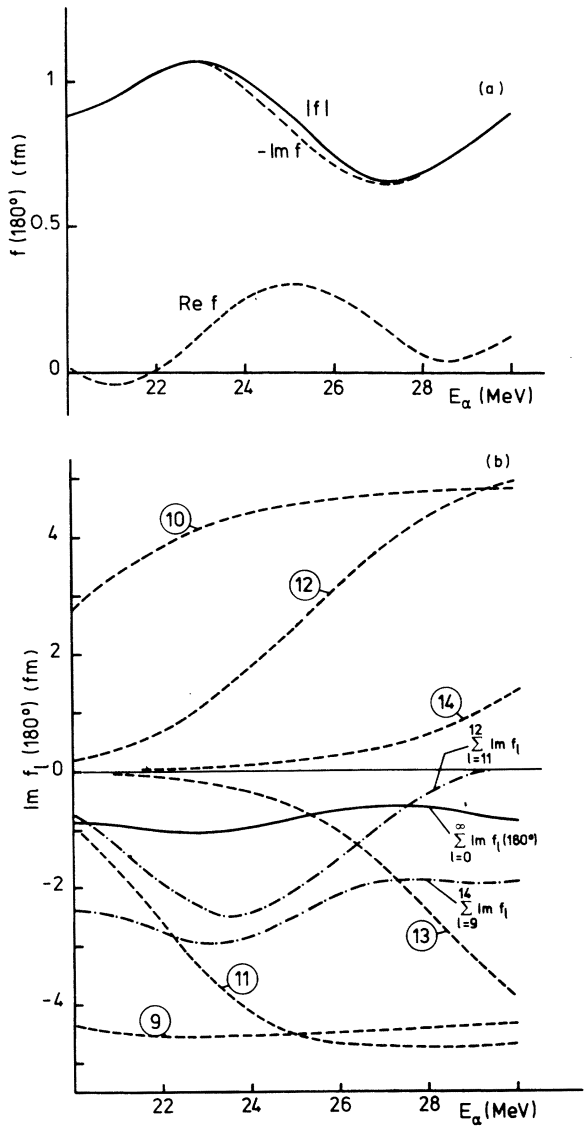

FIG. 9. (a) Decomposition of the backward elastic scattering amplitude in its real and imaginary parts as a function of energy. (b) Decomposition of the imaginary part of the backward elastic scattering amplitude into its various angular momentum components as a function of energy.

pendent optical model picture, the back-angle peaking results from a decreased absorption for surface partial waves, as compared with that used in the average potential of Gaul *et al.*[6] (this describes the "normal" scattering from heavier mass targets). In our model, the partial wave amplitudes differ from those of this latter potential for all l values; in fact, our total reaction cross section is even somewhat larger than that computed from the Gaul potential. Our results thus do not seem to substantiate the hypothesis relating ALAS to an angular momentum mismatch between the elastic and nonelastic channels.[49]

III. ANALYSIS OF THE INELASTIC SCATTERING DATA

A further test of the validity of the present optical model approach consists in applying it to the study of inelastic transitions in ^{40}Ca. The available data including large angle inelastic cross section (Schmeing and Santo,[16] Trombik, Eberhard, and Eck,[17] and also the new measurements taken at Louvain-la-Neuve[18]) indicate a back-angle increase for the low spin 0^+ [16-18] and 1^- [16,17] states. In particular, the cross sections for excitation of the lowest 0^+ states show, for energies ranging between 24 and 40 MeV, a large angle behavior which is very close to that for elastic scattering. No notable back enhancement seems to be present for other states (with a possible exception for the 6.29 MeV 3^- state at an impact energy of 29 MeV[16]), although the large angle cross sections remain well above those predicted by a DWBA calculation using a usual optical potential, e.g., the above-mentioned potential of Gaul *et al.*[6] A distinctive feature of the 3^- state at 3.73 MeV in the large angle region is the presence of a well marked, broad maximum of the differential cross section centered between $\theta = 165°$ and $\theta = 170°$.

The most interesting object for our purpose is the 3^- state at 3.73 MeV excitation energy. Indeed, the collective vibrational nature of this state seems to be well established,[50,51] it is strongly excited and fairly well separated in energy from neighboring states to which it appears to be only weakly coupled.[17,52,53] As a consequence, we expect the DWBA approximation, assuming a collective inelastic form factor,[54] to be valid; the resulting inelastic scattering cross sections should thus mainly reflect the properties of the optical potential which was used to generate the distorted waves and the complex inelastic form factor.[54] Our results, obtained using the code DWUCK,[55] with suitable modification to allow the use of potentials of the form of (1) and (2), are shown in Figs. 10–12, where they are seen to be in good agreement with the experimental data[16,18]: the angular behavior is well described at $E_\alpha = 24$, 29, and 40 MeV, and the sudden change observed between $E_\alpha = 40$ and 46 MeV is qualitatively reproduced. Results obtained from the average potential of Gaul *et al.*[6] are also shown in Fig. 10 for comparison: they fall much lower than experiment at large scattering angles. Values extracted for the parameter β_l [54] at $E_\alpha = 24$ and 29 MeV are compared in Table I with those deduced from DWBA analyses of the excitation of the same

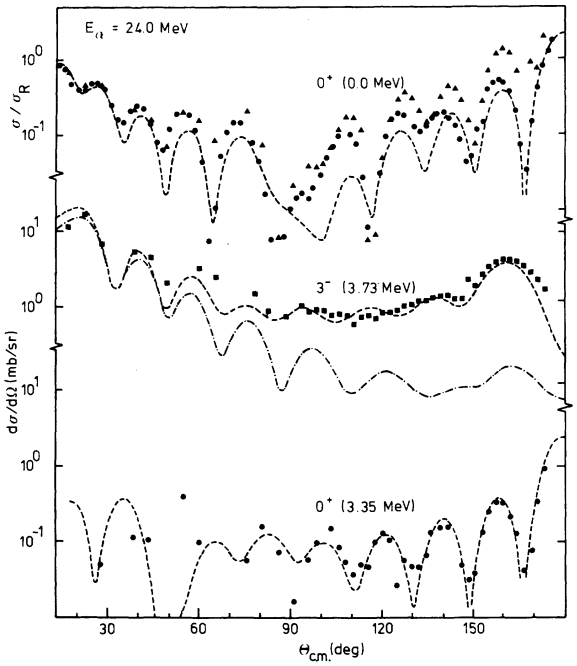

FIG. 10. α-^{40}Ca elastic and inelastic differential cross sections at $E_\alpha = 24$ MeV. Dashed curves were generated from the potential of (4) and (5); the dashed-dotted curve from the potential of Gaul *et al.* (Ref. 6). Experimental data: inelastic, Ref. 17; elastic, Ref. 17 (triangles), Ref. 6 (dots).

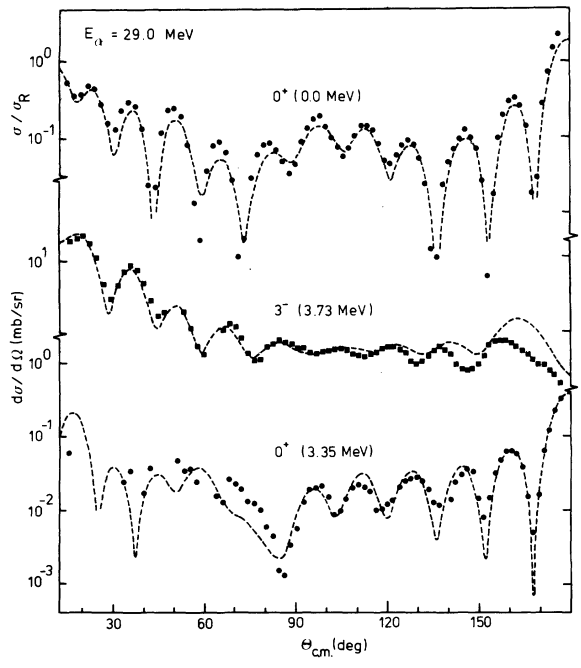

FIG. 11. Comparison of the predictions of the potential of (4) and (5) with the experimental data at $E_\alpha = 29$ MeV (Ref. 16).

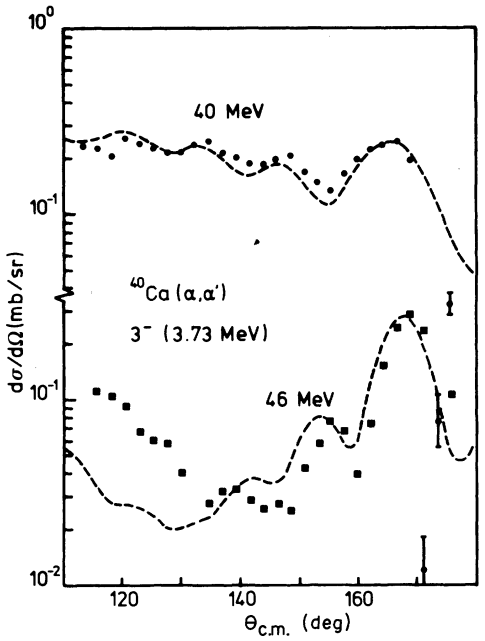

FIG. 12. Comparison of DWBA calculations using the potential of (4) and (5) with experimental data of the Louvain-la-Neuve–Cracow–Munich collaboration (Ref. 18) at $E_\alpha = 40$ and 46 MeV.

level by various projectiles.[31,50,52,56-58] The slight disagreement between our β_l values at 24 and 29 MeV is probably related to important discrepancies between the experimental elastic scattering data from different groups (see Fig. 10) which might also affect measurements in the inelastic channels. The important fluctuations put in evidence in a recent study by Eberhard *et al.*[8] could partly explain these differences. Our β_l values at $E_\alpha = 40$ MeV and $E_\alpha = 46$ MeV (0.18 and 0.26, respectively) are less satisfactory, as a consequence of the gradual degradation of the validity of the optical potential as energy increases. The cross sections for excitation of the 0^+ state at 3.35 MeV are also shown in Figs. 10 and 11. This state has been described as a 4p-4h configuration which supports a rotational band including the 2^+ and 4^+ states at 3.90 and 5.28 MeV.[59-62] Consequently, it cannot be accounted for by our model, the inadequacy of which is probably reflected by the large variations of β_l with energy (Table I). In fact, the good agreement between experiment and our (relative) large angle cross sections persists when large variations are imposed on the collective inelastic form factor, because the localization of this factor in r space, together with the strong absorption of low-l partial waves, selects a small number of partial wave amplitudes peaked around $l = 10$ at $E_\alpha = 24$–29 MeV. As a consequence, the

TABLE I. Deformation parameters β_l for α-particle excitation of ^{40}Ca, as obtained from a DWBA analysis using the potential of (4) and (5), compared with previously published values.

J^π (excitation energy)	Reference	Present work		50	56	31	52	57	58
	Lab energy (MeV)	24	29	31	96	100	24–31	55	12.8
	process	(α,α')		(α,α')	(α,α')	(α,α')	(α,α')	(p,p')	(d,d')
0^+ (3.35 MeV)		0.03	0.015						0.05–0.08
3^- (3.73 MeV)		0.28	0.24	0.24	0.24	0.25	0.25–0.25	0.33	0.30–0.32
5^- (4.49 MeV)		0.17	0.13	0.13			0.16–0.14	0.17	0.13–0.16

angular distribution for $\theta \gtrsim 110°$ is nearly proportional to the square of a Legendre polynomial of order 10—and also to the elastic cross section, as discussed in connection with Eq. (8). This behavior persists at the higher energies (40 and 46 MeV), the dominant l value increasing roughly like $(E_\alpha)^{1/2}$, as could be expected.

The collective DWBA model is less suitable to describe the excitation of other levels in ^{40}Ca, except in the small scattering angle region where good agreement with experiment is obtained, yielding β_l values which agree well with previously published ones. Some of these are given in Table I. This merely reflects the well-known model independence of the small angle DWBA excitation cross sections for inelastic α-nucleus scattering,[51] while the failure at large angles must be attributed to the nonapplicability of the collective picture, or to important couplings to other reaction channels.

IV. CONCLUSIONS

The feasibility of an optical model description of the anomalous large angle scattering for α-^{40}Ca at low energies (20 MeV $\leq E_\alpha \leq$ 50 MeV) has been demonstrated. To this end, a fit to experiment was performed at a single energy (E_α = 29 MeV) and a single parameter of the resulting potential (the imaginary part radius) was thereafter allowed to vary with energy. It has been shown that this potential gives a good description of the characteristic energy behavior of the large angle differential cross sections in the investigated energy range.

Examination of the corresponding reflection coefficients reveals the nonresonant nature of the phenomenon; an interpretation of the "rotational band" behavior of the large angle elastic cross sections in terms of strong absorption has been suggested.

Finally, a DWBA analysis of some inelastic transitions using the same potential has been carried out. The predictions of the calculations for the strongly excited collective 3^- state at 3.73 MeV are in good agreement with experiment over the whole angular range; the extracted deformation parameter is consistent with previous estimates.

ACKNOWLEDGMENTS

Special thanks are due Professor G. Grégoire for communication of new unpublished data, and to Professor K. A. Eberhard, Professor K. Grotowski, Professor R. Santo, and Professor R. Stock for providing us with their data. Very interesting discussions with our colleagues at Louvain-la-Neuve, as well as with Professor K. Grotowski, Professor R. Ceuleneer, and Dr. M. Erculisse, are gratefully acknowledged.

*Chercheur de l'Institut Interuniversitaire des Sciences Nucléaires.

[1]Proceedings of the Symposium on Four Nucleon Correlations and Alpha Rotator Structure, Marburg, Germany, October 30–November 2, 1972, edited by R. Stock (unpublished), p. 115ff.

[2]Proceedings of the First Louvain-Cracow Seminar on the Alpha-Nucleus Interaction, Cracow, Poland, 6–9 November, 1973 (unpublished), INP870/PL.

[3]P. C. Macq *et al.* (unpublished).

[4]C. R. Gruhn and N. S. Wall, Nucl. Phys. 81, 161 (1966).

[5]R. Stock, G. Gaul, R. Santo, M. Bernas, B. Harvey, D. Hendrie, J. Mahoney, J. Sherman, J. Steyaert, and M. Zisman, Phys. Rev. C 6, 1226 (1972).

[6]G. Gaul, H. Lüdecke, R. Santo, H. Schmeing, and R. Stock, Nucl. Phys. A137, 177 (1969).

[7]A. Gobbi, R. Wieland, L. Chua, D. Shapira, and D. A. Bromley, Phys. Rev. C 7, 30 (1973).

[8]K. A. Eberhard, T. H. Braid, T. Renner, J. P. Schiffer, and S. Vigdor, Phys. Rev. C 14, 548 (1976).

[9]L. McFadden and G. R. Satchler, Nucl. Phys. 84, 177 (1966).

[10]E. Labie, J. Lega, and P. C. Macq, Nucl. Phys. A135, 145 (1969).

[11]A. Budzanowski, A. Dudek, R. Dymarz, K. Grotowski, L. Jarczyk, H. Niewodniczanski, and A. Strzalkowski, Nucl. Phys. A126, 369 (1969).

[12]A. Bobrowska, A. Budzanowski, K. Grotowski,

L. Jarczyk, B. Kamys, S. Micek, M. Polok, A. Strzalkowski, and Z. Wrobel, Institute for Nuclear Physics, Internal Report No. INP777/PL, Cracow, 1971 (unpublished).
[13]F. Michel, Phys. Lett. 60B, 229 (1976).
[14]N. C. Schmeing, Nucl. Phys. A142, 449 (1970).
[15]H. Oeschler, H. Schröter, H. Fuchs, L. Baum, G. Gaul, H. Lüdecke, R. Santo, and R. Stock, Phys. Rev. Lett. 26, 694 (1972).
[16]H. Schmeing and R. Santo, Phys. Lett. 33B, 219 (1970).
[17]W. Trombik, K. A. Eberhard, and J. S. Eck, Phys. Rev. C 1, 685 (1975).
[18]Louvain-la-Neuve–Cracow–Munich collaboration (unpublished data).
[19]E. T. Boschitz, J. S. Vincent, R. W. Bercaw, and J. R. Priest, Phys. Rev. Lett. 13, 442 (1964).
[20]A. Budzanowski, K. Grotowski, L. Jarczyk, B. Lazarska, S. Micek, H. Niewodniczanski, A. Strzalkowski, and Z. Wrobel, Phys. Lett. 16, 135 (1965).
[21]J. Lega and P. C. Macq, J. Phys. 32, 369 (1971).
[22]J. Schiele (private communication).
[23]T. Delbar, G. Grégoire, J. Lega, G. Paic, C. Pirart, P. Wastyn, R. Ceuleneer, and F. Michel, contribution to the International Conference on Radial Shape of Nuclei, Cracow, Poland, 22–25 June 1976 (unpublished), Vol. 1E, p. 105.
[24]D. C. Weisser, J. S. Lilley, R. K. Hobbie, and G. W. Greenlees, Phys. Rev. C 2, 544 (1970).
[25]A. Budzanowski, K. Grotowski, M. Grzywacz, and A. Strzalkowski, Internal Report, Cracow, 1971 (unpublished).
[26]A. Budzanowski, K. Grotowski, Z. Majka, and A. Strzalkowski, in Proceedings of the European Conference on Nuclear Physics with Heavy Ions, Caen, France, 6–10 September 1976 (unpublished).
[27]D. A. Goldberg, Phys. Lett. 55B, 59 (1975).
[28]K. Grotowski (private communication).
[29]P. Mailandt, J. S. Lilley, and G. W. Greenlees, Phys. Rev. C 8, 2189 (1973).
[30]F. Michel, Phys. Rev. C 13, 1446 (1976).
[31]H. Eickhoff, D. Frekers, H. Löhner, H. Poppensieker, R. Santo, G. Gaul, C. Mayer-Böricke, and P. Turek, Nucl. Phys. A252, 333 (1975).
[32]D. M. Brink and N. Takigawa, Nucl. Phys. A279, 159 (1977).
[33]P. P. Singh, L. W. Put, and A. M. J. Paans, in *Proceedings of the International Conference on Nuclear Physics, Munich, 1973,* edited by J. de Boer and H. J. Mang (North-Holland, Amsterdam/American Elsevier, New York, 1973), Vol. 1, p. 337.
[34]P. P. Singh and P. Schwandt, Phys. Lett. 42B, 181 (1972); P. P. Singh, P. Schwandt, and G. C. Yang, Phys. Lett. 59B, 113 (1975).
[35]D. A. Goldberg and S. M. Smith, Phys. Rev. Lett. 29, 500 (1972).
[36]A. Budzanowski, K. Chyla, R. Czabanski, K. Grotowski, L. Jarczyk, B. Kamys, A. Kapuscik, S. Micek, J. Ploskonka, A. Strzalkowski, J. Szmider, Z. Wrobel, L. Zastawniak, and R. Zybert, Nucl. Phys. A211, 463 (1973).
[37]P. C. Macq, A. Budzanowski, H. Dabrowski, L. Freindl, K. Grotowski, S. Micek, R. Planeta, and A. Strzalkowski (unpublished).
[38]W. E. Frahn and R. H. Venter, Ann. Phys. (N.Y.) 24, 243 (1963).
[39]F. Michel, Ph.D. thesis, University of Mons, 1976 (unpublished).
[40]D. M. Brink, J. Grabowski, and E. Vogt (unpublished).
[41]A. S. Rinat, Phys. Lett. 38B, 281 (1972).
[42]H. Friedrich, K. Langanke, A. Weiguny, and R. Santo, Phys. Lett. 55B, 345 (1975).
[43]H. Friedrich and K. Langanke, Nucl. Phys. A252, 47 (1975).
[44]D. Agassi and N. S. Wall, Phys. Rev. C 7, 1368 (1973).
[45]A. Budzanowski, Ref. 1, p. 148.
[46]B. Fernandez and J. S. Blair, Phys. Rev. C 1, 523 (1970).
[47]D. F. Jackson and C. G. Morgan, Phys. Rev. 175, 1402 (1968).
[48]J. C. Faivre, H. Krivine, and A. M. Papiau, Nucl. Phys. A108, 508 (1968).
[49]K. A. Eberhard, Phys. Lett. 33B, 343 (1970).
[50]E. P. Lippincott and A. M. Bernstein, Phys. Rev. 163, 1170 (1967).
[51]A. M. Bernstein, in *Advances in Nuclear Physics*, edited by M. Baranger and E. Vogt (Plenum, New York, 1969), Vol. 3, p. 325.
[52]M. J. A. de Voigt, D. Cline, and R. N. Horoshko, Phys. Rev. C 10, 1798 (1974).
[53]J. G. Cramer, K. A. Eberhard, and W. Trombik, Phys. Rev. C 8, 625 (1973).
[54]N. Austern, *Direct Nuclear Reaction Theories* (Wiley, New York, 1970).
[55]P. D. Kunz, code DWUCK, University of Colorado, 1969 (unpublished).
[56]D. H. Youngblood, J. M. Moss, C. M. Rosza, J. D. Bronson, A. D. Bacher, and D. R. Brown, Phys. Rev. C 13, 994 (1976).
[57]K. Yagi, H. Ejiri, M. Furukawa, Y. Ishizaki, M. Koike, K. Matsuda, J. Nakajima, E. Nonaka, Y. Saji, E. Tanaka, and G. R. Satchler, Phys. Lett. 10, 186 (1964).
[58]H. Niewodniczanski, J. Nurzynski, A. Strzalkowski, and G. R. Satchler, Phys. Rev. 146, 799 (1966).
[59]W. J. Gerace and A. M. Green, Nucl. Phys. A123, 241 (1969).
[60]T. R. Canada, R. S. Cox, J. S. Duval, C. H. Sinex, and C. M. Class, Phys. Rev. 188, 1741 (1969).
[61]J. R. McDonald, D. H. Wilkinson, and D. E. Alburger, Phys. Rev. C 3, 219 (1971).
[62]P. Braun-Munziger, C. K. Gelbke, N. Grama, H. Homeyer, E. Ridinger, and R. Stock, Phys. Rev. Lett. 29, 1261 (1972).